J|A|C|S
ARTICLES
Published on Web 09/03/2004

Activation of Molecular Hydrogen over a Binuclear Complex with Rh_2S_2 Core: DFT Calculations and NMR Mechanistic Studies

Andrea Ienco,[†] Maria José Calhorda,[‡] Joachim Reinhold,[§] Francesca Reineri,[||] Claudio Bianchini,[†] Maurizio Peruzzini,[†] Francesco Vizza,[†] and Carlo Mealli*,[†]

Contribution from the Istituto di Chimica dei Composti OrganoMetallici (ICCOM), CNR, Via Madonna del Piano, I-50019 Sesto Fiorentino (Firenze), Italy, ITQB, Av da República Apart 127, EAN, 2781-901 Oeiras, and Departimento Química e Bioquímica, FC, Universidade de Lisboa, 1749-016 Lisboa, Portugal, Wilhelm Ostwald Institut für Physikalische und Theoretische Chemie, Universität Leipzig, D-04103 Leipzig, Germany, and Dipartimento di Chimica Inorganica, Chimica Fisica e Chimica dei Materiali, Università di Torino, Via Pietro Giuria 7, I-10125 Torino, Italy

Received April 7, 2004; E-mail: carlo.mealli@iccom.cnr.it

Abstract: The dicationic complex $[(triphos)Rh(\mu\text{-}S)_2Rh(triphos)]^{2+}$, **1** (modeled as **1c**) [triphos = $CH_3C(CH_2PPh_2)_3$], is known to activate two dihydrogen molecules and produce the bis(μ-hydrosulfido) product $[(triphos)(H)Rh(\mu\text{-}SH)_2Rh(H)(triphos)]^{2+}$, **2** (modeled as **2b**), from which **1** is reversibly obtained. The possible steps of the process have been investigated with DFT calculations. It has been found that each d^6 metal ion in **1c**, with local square pyramidal geometry, is able to anchor one H_2 molecule in the side-on coordination. The step is followed by heterolytic splitting of the H−H bond over one adjacent and polarized Rh−S linkage. The process may be completed before the second H_2 molecule is added. Alternatively, both H_2 molecules are trapped by the Rh_2S_2 core before being split in two distinct steps. Since the ambiguity could not be solved by calculations, ^{31}P and ^1H NMR experiments, including para-hydrogen techniques, have been performed to identify the actual pathway. In no case is there experimental evidence for any Rh−(η^2-H_2) adduct, probably due to its very short lifetime. Conversely, ^1H NMR analysis of the hydride region indicates only one reaction intermediate which corresponds to the monohydride-μ-hydrosulfide complex $[(triphos)Rh(H)(\mu\text{-}SH)(\mu\text{-}S)Rh(triphos)]^{2+}$ (**3**) (model **5a**). This excludes the second hypothesized pathway. From an energetic viewpoint the computational results support the feasibility of the whole process. In fact, the highest energy for H_2 activation is 8.6 kcal mol^{-1}, while a larger but still surmountable barrier of 34.6 kcal mol^{-1} is in line with the reversibility of the process.

Introduction

Activation of molecular hydrogen by transition-metal complexes is a problem of major importance in chemistry,[1] biology,[2] and industrial applications. In the latter respect, the topic has recently acquired additional interest for the potential usage of metallorganic frameworks in hydrogen storage.[3] This type of chemistry has also inspired fundamental studies in the last 20 years.[1] In particular, the discovery that some metalloenzymes deal with the transformation of hydrogen has led to blossoming interest about the biological aspects of the process. These enzymes include the hydrogenases, which reversibly catalyze the transformation of H_2 in H^+, and the nitrogenases, which produce NH_3 from dinitrogen and dihydrogen.[4] Biological activation of H_2 in these metalloenzymes usually takes place at binuclear metal centers and involves sulfur ligands. There are some hydrogenases that only contain iron, while others are mixed (Fe−Ni hydrogenase). The latter have been the subject of many theoretical studies,[5] especially after a crystal structure determination showed the presence of carbonyl and cyanide

[†] Istituto di Chimica dei Composti Organometallici.
[‡] ITQB and Universidade de Lisboa.
[§] Universität Leipzig.
[||] Università di Torino.

(1) (a) *Recent Advances in Hydride Chemistry*; Peruzzini, M., Poli, R., Eds.; Elsevier SA: Amsterdam, The Netherlands, 2001. (b) *Metal Dihydrogen and s-Bond Complexes*; Kubas, G. J., Ed.; Kluwer Academic/Plenum Publishers: New York, 2001. (c) *Transition Metal Hydrides;* Dedieu, A., Ed.; VCH Publishers: New York, 1991.
(2) (a) Adams, M. W. W.; Stiefel, E. I. *Curr. Opin. Chem. Biol.* **2000**, *4*, 214. (b) Rees, R. K. *Annu. Rev. Biochem.* **2002**, *71*, 221.
(3) Rosi, N. L.; Eckert, J.; Eddaoudi, M.; Vodak, D. T.; Kim, J.; O'Keeffe, M.; Yaghi, O. M. *Science* **2003**, *300*, 1127.
(4) (a) Henderson, R. A. In *Recent Advances in Hydride Chemistry*; Peruzzini, M., Poli, R., Eds.; Elsevier SA: Amsterdam, The Netherlands, 2001; Chapter 16. (b) Cammack, R.; van Vliet, P. In *Bioinorganic Catalysis;* Reedijk, J., Bouwman, E., Eds.; Marcel Dekker: New York, 1999; Chapter 9.
(5) (a) Niu, S.; Thomson, L. M.; Hall, M. B. *J. Am. Chem. Soc.* **1999**, *121*, 4000. (b) Niu, S.; Hall, M. B. *Inorg. Chem.* **2001**, *40*, 6201. (c) Foerster, S.; Stein, M.; Brecht, M.; Ogata, H.; Higuchi, Y.; Lubitz, W. *J. Am. Chem. Soc.* **2003**, *125*, 83. (d) Stein, M.; van Lenthe, E.; Baerends, E. J.; Lubitz, W. *J. Phys. Chem. A* **2001**, *105*, 416. (e) Pavlov, M.; Siegbahn, P. E. M.; Blomberg, M. R. A.; Crabtree, R. H. *J. Am. Chem. Soc.* **1998**, *120*, 548. (f) De Gioia, L.; Fantucci, P.; Guigliarelli, B.; Bertrand, P. *Inorg. Chem.* **1999**, *38*, 2658. (g) Nishibayashi, Y.; Iwai, S.; Hidai, M. *J. Am. Chem. Soc.* **1998**, *120*, 10559. (h) Zhou, T.; Mo, Y.; Liu, A.; Zhou, Z.; Tsai, K. R. *Inorg. Chem.* **2004**, *43*, 923.

10.1021/ja047992j CCC: $27.50

Scheme 1

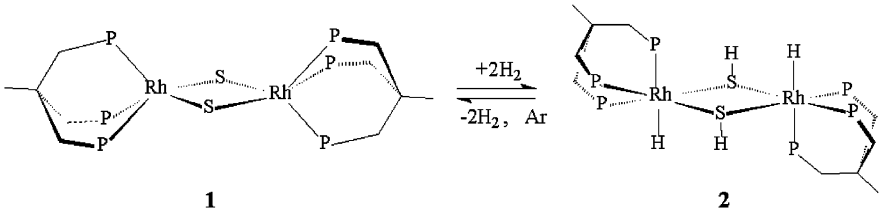

1 **2**

ligands in the coordination sphere of iron.[6] Even if the presence of the latter ligands does not totally exclude the attainment of high-spin states, the many experimental[7] and theoretical[8] studies, based on simple molecular models, have invariably considered diamagnetic, low-spin, species. Often, the biological active sites contain sulfur ligands, and involvement of dihydrogen implies the formation and/or cleavage of S−H bonds.[9] In this respect, such a reactivity is, at least, mechanistically related to the important industrial process of hydrodesulfurization by which sulfur is removed from fossil fuels.[10] Also, modeling of the dihydrogen activation by transition-metal species has often involved sulfide compounds with metal(s) in high oxidation states that force the heterolytic H^-/H^+ splitting. Conversely, the homolytic H−H cleavage, through oxidative addition, usually requires metal(s) in lower oxidation states.[11] Most of these processes have received much attention from a theoretical viewpoint also, a good reference being the review of Niu and Hall.[12]

The coordinatively unsaturated dimeric rhodium system $[(triphos)Rh(\mu\text{-}S)_2Rh(triphos)]^{2+}$, **1** [triphos = $CH_3C(CH_2\text{-}PPh_2)_3$], was found to activate dihydrogen reversibly and heterolytically.[13] The process is shown in Scheme 1.[14] Although the final product $[(triphos)(H)Rh(\mu\text{-}SH)_2Rh(H)(triphos)]^{2+}$, **2**, has been structurally characterized, there are only hypotheses regarding the structure of the reagent **1** and the proceeding of the reaction. For instances Morris suggested that a possible intermediate of the reaction is a species with a η^2-H_2-coordinated molecule at each metal center.[15] The acidity of the bis-(η^2-H_2) complex was supposed to be enough to generate the μ-SH ligand by heterolytic splitting of the H_2 ligand in the intermediate adduct.

Complex **1** is a very rare example of an organometallic compound where a naked sulfur ligand assists the heterolytic splitting of dihydrogen, a process which is relevant for both H_2 activation by metal sulfides and hydrogenases. In fact, only a handful of compounds are known to produce hydrosulfido complexes from H_2 activation, among them we recall Sellmann's 1,2-benzeneditiolate rhodium and ruthenium complexes,[16] Bergman's titanocene monosulfide derivatives $[Cp^*_2Ti(=S)(py)]$ and $[Cp^*_2Ti(\eta^2\text{-}S_2)]$,[17] and Rakowski-DuBois' $[\{CpMoS_x\}_y]$ polymers.[18] Particularly related to the present study is the work of Rauchfuss, who showed how the hydrido(hydrosulfide) complex $[Ir_2H_2(\mu\text{-}H)(\mu\text{-}SH)(\mu\text{-}S)(PPh_3)_4]$ is obtained from a double hydrogenation of the dinuclear iridium(II) complex $[Ir_2S_2\text{-}(PPh_3)_4]$.[19] In the stepwise process the first added H_2 molecule undergoes *homolytic cleavage* while the second process is purely *heterolytic*.

Initially, this study was essentially a theoretical one and focused on the following points: (i) determining the unknown structural aspects of the 32-electron complex reagent **1**, (ii) revising the controversial aspect of the X-ray structure of the product **2** which highlighted short contacts (∼1.90 Å) between the H atom of any SH bridge and the nearest hydride ligand while a direct interaction was excluded by specific calculations,[20] and (iii) outlining, by DFT calculations, the pathway of the double-hydrogenation reaction through characterization of the intermediate species and transition states. Since the computational approach could not solve all the ambiguities about reaction intermediates, further NMR investigation was planned also because of insufficient spectroscopic characterization in the original report.[13] Accordingly, we present complementary NMR data on the behavior of **2** as obtained from low-temperature and para-H_2 NMR experiments. In turn, these results have inspired new ideas for a finer computational analysis.

Results and Discussion

First, the structural features of the reagent and product of the hydrogenation reaction, namely, compounds **1** and **2** (see Scheme 1), will be discussed as well as of alternative conformers. Afterward, the reaction path and the transition states will be analyzed in detail.

(6) (a) Volbeda, A.; Piras, C.; Charon, M. H.; Hatchikian, E. C.; Frey, M.; Fontecilla Campos, J. C. *Nature* **1995**, *373*, 580. (b) Volbeda, A.; Garcin, E.; Piras, C.; de Lacey, A. L.; Fernandez, V. M.; Hatchikian, E. C.; Frey, M.; Fontecilla Campos, J. C. *J. Am. Chem. Soc.* **1996**, *118*, 12989. (c) Higuchi, Y.; Yagi, T.; Yasuoka, N. *Structure* **1997**, *5*, 1671.

(7) (a) Sellmann, D.; Rackelmann, G. B.; Heinemann, F. W. *Chem. Eur. J.* **1997**, *3*, 2071. (b) Sellmann, D.; Gottschalk-Gaudig, T.; Heinemann, F. W. *Inorg. Chem.* **1998**, *37*, 3982. (c) Sweeney, Z. K.; Polse, J. L.; Bergman, R. G.; Andersen, R. A. *Organometallics* **1999**, *18*, 5502. (d) Lawrence, J. D.; Li, H.; Rauchfuss, T. B.; Bénard, M.; Rohmer, M. M. *Angew. Chem., Int. Ed. Engl.* **2001**, *40*, 1768.

(8) (a) Pavlov, M.; Siegbahn, P. E. M.; Blomberg, M. R. A.; Crabtree, R. H. *J. Am. Chem. Soc.* **1998**, *120*, 548. (b) Niu, S.; Thomson, L. M.; Hall, M. B. *J. Am. Chem. Soc.* **1999**, *121*, 4000. (c) De Gioia, L.; Fantucci, P.; Guigliarelli, B.; Bertrand, P. *Inorg. Chem.* **1999**, *38*, 2658. (d) DuBois, M. R.; VanDerveer, M. C.; DuBois, D. L.; Haltiwanger, R. C.; Miller, W. K. *J. Am. Chem. Soc.* **1980**, *102*, 7456.

(9) For recent reviews on transition-metal hydrosulfides, see: (a) Peruzzini, M.; de los Rios, I.; Romerosa, A. *Prog. Inorg. Chem.* **2001**, *50*, 169. (b) Kuwata, S.; Hidai, M. *Coord. Chem. Rev.* **2001**, *213*, 211.

(10) (a) Topsøe, H.; Clausen, B. S.; Massoth, F. E. In *Hydrotreating Catalysis, Science and Technology*; Anderson, J. R., Boudart, M., Eds.; Springer-Verlag: Berlin/New York, 1996; Vol 11. (b) Schwarz, D. E.; Dopke, J. A.; Rauchfuss, T. B.; Wilson, S. R. *Angew. Chem., Int. Ed. Engl.* **2001**, *40*, 2351. (c) Byskov, L. S.; Nørskov, J. K.; Clausen, B. S.; Topsøe, H. *J. Catal.* **1999**, *187*, 109.

(11) Halpern, J. *Inorg. Chim. Acta* **1985**, *100*, 41.

(12) Niu, S.; Hall, M. B. *Chem. Rev.* **2000**, *100*, 353.

(13) Bianchini, C.; Mealli, C.; Meli, A.; Sabat, M. *Inorg. Chem.* **1986**, *25*, 4618.

(14) An alternative synthesis of **2**, involving the hydrogenation of a rhodium dithiocarbonate species and the elimination of 1 equiv of COS, has been also described: Bianchini, C.; Meli, A. *Inorg. Chem.* **1987**, *26*, 4268.

(15) (a) Morris, R. H. *Inorg. Chem.* **1992**, *31*, 1471. (b) Morris, R. H. In *Transition Metal Sulfides*; Weber, T., Prins, R., van Santen, R. A., Eds.; Kluwer: The Netherlands, 1998.

(16) See: Sellmann, D.; Sutter, J. *Prog. Inorg. Chem.* **2004**, *52*, 585 and references therein.

(17) Sweeny, Z. K.; Polse, J. L.; Bergman, R. G.; Andersen, R. A. *Organometallics* **1999**, *18*, 5502.

(18) Rakowski DuBois, M.; VanDerveer, M. C.; DuBois, D. L.; Haltiwanger, R. C.; Miller, W. K. *J. Am. Chem. Soc.* **1980**, *102*, 7456. Rakowski DuBois, M.; VanDerveer, M. C.; DuBois, D. L.; Haltiwanger, R. C.; Miller, W. K. *Chem. Rev.* **1989**, *89*, 1 and references therein.

(19) (a) Linck, R. C.; Pafford, R. J.; Rauchfuss, T. B. *J. Am. Chem. Soc.* **2001**, *123*, 8856. (b) Rauchfuss, T. B. *Inorg. Chem.* **2004**, *43*, 14.

(20) Braga, D.; Grepioni, F.; Tedesco, E.; Calhorda, M. J.; Lopes, P. E. M. *New J. Chem.* **1999**, *23*, 219.

1. Modeling of the Reagent $[RhL_3(\mu\text{-}S)]_2^{2+}$. This species belongs to the rich family of dimers with general formula $[ML_n(\mu\text{-}X)]_2^{m+}$ (X = naked chalcogenide) with M_2X_2 frameworks, which have been analyzed in some detail by means of EHMO calculations and perturbation theory principles.[21] There is at least one X-ray structure available for different combinations of M, L, *n*, and *m*+ with the exception of 32-electron species of which the Rh(III) derivative **1** represents a relevant example. Although a M═M double bond is predicted for the latter on the basis of the effective atomic number rule[22] (EAN), it will be shown that this is not actually the case.

In the absence of precise structural information for **1**, two alternative conformations were selected for a model with three discrete PH_3 terminal ligands at each metal. In Scheme 2 the expected staggered (C_{2v}, **1a**) or eclipsed (C_{2h}, **1b**) geometries are presented.

Scheme 2

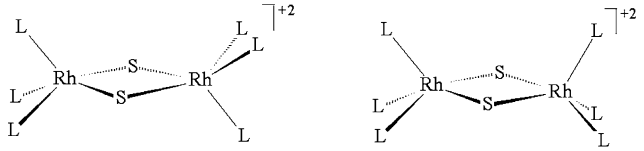

1a **1b**

None of the computed stationary points **1c** and **1d** (Scheme 3) has a pseudo-3-fold axis through the $L_3Rh\cdots RhL_3$ grouping as occurs for comparable 34-e species[23,24] (see also Supporting Information). In fact, both structures have local square pyramidal environments at the metals.

Scheme 3

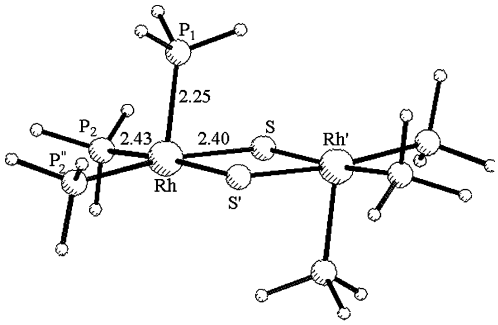

1c

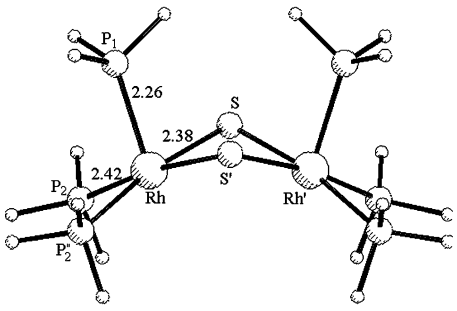

1d

The general MO picture of these systems has been previously reported.[21] Given the d^6 electron count of each metal, there are two isolated LUMOs (*in phase* and *out of phase* combinations of σ metal hybrids trans to the P_1 donors) that confer strong electrophilicity to the metal atoms. However, the sulfur bridges, by drifting some of their electron density, compensate in part for the vacancy of these orbitals (vide infra).

Structure **1d** is more stable than **1c** by 7.3 kcal mol^{-1}, but it may be excluded that the puckering (bending at the S−S line = 138°) originates from an incipient Rh−Rh bent bonding. In fact, the intermetallic separation is quite long (3.20 Å), and there is no electron pair available to populate the bonding combination of σ hybrids. Moreover, no bent geometry of type **1d** has ever been ascertained for dimers with terminal triphos ligands on account of the steric hindrance between the six bulky phenyl substituents that wrap the metal atoms. Qualitative MO arguments, based on EHMO calculations (see Supporting Information), account well for the larger stability of the bent (**1d**) vs planar conformer (**1c**). On the other hand, use of the simplified tripodal ligand $HC(CH_2PH_2)_3$ allowed only optimization of conformer **1e** (Scheme 4), which has an extended planar skeleton $P_2Rh(\mu\text{-}S)_2RhP_2$ with additional Rh−P axial bonds. The latter are about 0.2 Å shorter than the equatorial ones, while the Rh−S distances are all close to 2.40 Å. Thus, also in view of the geometrical consistency, the simpler precursor **1c** was considered reliable for studying the double-hydrogenation reaction.

Scheme 4

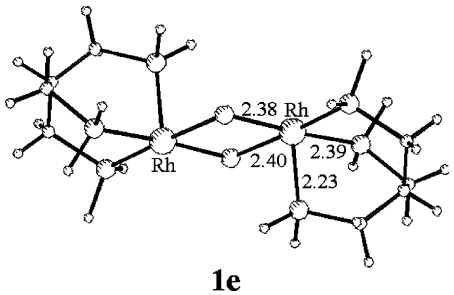

1e

Finally, it is noteworthy that the LUMO and LUMO+1 levels of **1c** are *in-phase* and *out-of-phase* combinations of the σ metal hybrids which point toward the sixth and empty octahedral position. Importantly, the LUMO+1, depicted in Scheme 5, highlights the interaction of the empty z^2-based metal orbitals with the sulfur p_π ones. This suggests a $S_2\rightarrow Rh_2$ two-electron donation which accounts well for the relative stability of the 32-electron species in the absence of a direct Rh−Rh bond. Despite a nonoptimum overlap, the electron density received by the empty z^2 metal orbitals permits formal attainment of the 18-electron configuration for each metal and confer an order of 1.5 to each Rh−S bond.

In the literature the only other Rh(III) binuclear derivative with stereochemical and electronic features comparable to the present unusual system **1** is $[Rh(\mu\text{-}C_7H_4NS_2)(COCH_3)(I)$-

Scheme 5

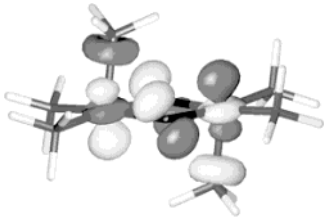

LUMO+1

$(PPh_3)]_2$.[25] In Ciriano's compound the Rh atoms, with three terminal ligands each, are bridged by the exocyclic sulfur atoms of two $C_7H_4NS_2$ ligands (see Scheme 6).

Scheme 6

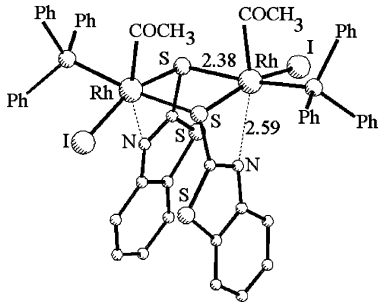

In this case the metal is not totally unsaturated since the endocyclic nitrogen atoms of the bridging mercaptobenzothiazoles seem to complete a distorted octahedral coordination sphere despite the rather long Rh···N separations (2.59 Å).

2. Modeling of the Final Product $[RhHL_3(\mu\text{-}SH)]_2^{2+}$. Two optimized C_i models of the final product **2** (reaction of Scheme 1) are presented in Scheme 7 (distances in Å).

Scheme 7

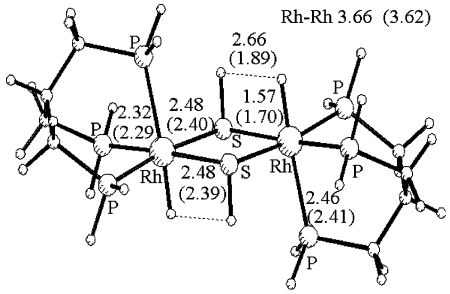

2a

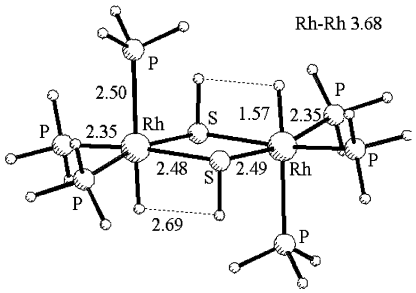

2b

First, the geometry of the experimental structure,[13] with the phenyl groups replaced by hydrogen atoms, was considered (complex **2a**). The bond distances from the X-ray determination of **2** (reported in parentheses) agree satisfactorily with the computed ones. There is only a major discrepancy in the separation between the H atoms of the activated H_2 molecules (dashed lines in Scheme 7) as, most probably, the distance of 1.89 Å is underestimated in the X-ray structure. This is supported by the H(hydride)−H(S) separation of 2.62 Å (very close to the 2.66 Å value in **2a**) determined for the similar structure of $[RhHCl(PPh_3)_2(\mu\text{-}SH)]_2$, where a chloride ion replaces one of the phosphorus donors.[26] In light of these results, the previous hypothesis[20] of a persisting $H^+\cdots H^-$ ionic interaction in **2**, which eventually facilitates H_2 recoupling, seems unlikely.

Next, a full geometry optimization (again with C_i symmetry) was performed for the simpler model **2b** with discrete PH_3 ligands. Good agreement with the experimental data as well as with the calculated parameters of **2a** is found. Also, from an energetic point of view, the addition of two H_2 molecules to the precursor **1e** to form **2b** is comparable to that transforming **1c** into **2b** (−45.8 and −47.6 kcal mol^{-1}, respectively), so that the tripodal ligand was dismissed in the computational study of the reactivity.

3. Modeling of Reaction Intermediates and Transition States. The simultaneous activation of two dihydrogen molecules by the reagent **1** to form product **2** in one step is a kinetically improbable reaction. Were any termolecular reaction feasible, one could think of an Rh_2S_2 quadrupole polarizing two distinct H_2 molecules, as shown in Scheme 8. In fact, the highly polarized Rh−S linkages could promote H−H heterolytic splittings. As an alternative and more realistic mechanism, the unsaturated metal centers can provide the driving force to bind the H_2 molecules. Computational analysis allows one to establish that the approach of dihydrogen is stepwise and that the target is invariably the metal center.

Scheme 8

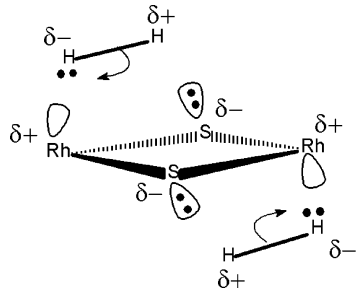

3.1. Structural Key Points in the Approach of the First H_2 Molecule to Model 1c. By using a combined method for determining reaction path minima and transition-state geometries,[27] the approach of one H_2 molecule to the Rh_2S_2 rhombus was systematically explored. In this manner, it was found that the H_2 molecule arrives, almost intact, directly over the sixth available octahedral position of one metal and generates the monoadduct $[RhL_3(\mu\text{-}S)_2L_3(\eta^2\text{-}H_2)Rh]^{2+}$, **4** (shown at the top of Scheme 9). The latter, an actual minimum, may be considered as the first intermediate in the hydrogenation process. From an energetic viewpoint, formation of **4** is slightly exothermic as the computed energy gain with respect to the isolated reagents **1c** and H_2 is only 0.3 kcal mol^{-1}. Despite the flat potential-energy surface (PES), it has been possible to locate the transition state, $\mathbf{1c_{TS}}$ (bottom of Scheme 9) at a separation between H_2 and the metal of about 4 Å and with an activation energy of

(21) Mealli, C.; Orlandini, A. In *Metal Clusters in Chemistry*; Braunstein, P., Oro, L., Raithby,P., Eds.; Wiley-VCH: Weinheim, 1999; pp 143−162.
(22) See, for instance: Mingos, D. M. P.; Wales, D. J. In *Introduction to Cluster Chemistry*; Prentice Hall: Englewood Cliffs, NJ, 1990.
(23) Ghilardi, C. A.; Mealli, C.; Midollini, S.; Nefedov, V. I.; Orlandini, A.; Sacconi, L. *Inorg. Chem.* **1980**, *19*, 2454.
(24) Klein, H. F.; Gass, M.; Koch, U.; Eisenmann, B.; Schäfer, H. *Z. Naturforsch.* **1988**, *43b*, 830.
(25) Ciriano, M. A.; Pérez-Torrente, J. J.; Lahoz, F. J.; Oro, L. *J. Organomet. Chem.* **1994**, *482*, 53.
(26) Mueting, A. M.; Boyle, P.; Pignolet, L. H. *Inorg. Chem.* **1984**, *23*, 44.
(27) Ayala, P. Y.; Schlegel, H. B. *J. Chem. Phys.* **1997**, *107*, 375.

Scheme 9

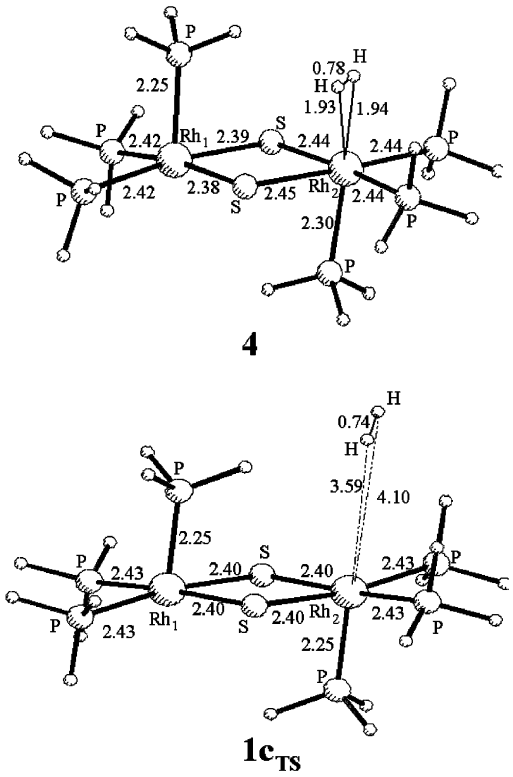

only 0.4 kcal mol^{-1}. Although the Gibbs free energy is slightly larger (3.6 kcal mol^{-1} at room temperature), the computed values remain too small to be significant. On the other hand, the same problem was reported by other authors who could not locate the transition state for the addition of H_2 to $Rh(CO)_3(CHO)$ and concluded that the reaction, although exothermic by 3.1 kcal mol^{-1}, proceeds without a barrier.[28]

Some geometrical features of **4** deserve comment. The primary geometry of the dehydrogenated precursor **1c** is maintained, but there is an evident trans influence of the dihapto-coordinated H_2 molecule. The Rh2−P_{ax} bond, opposite the σ-bonded H_2 ligand, is in fact 0.05 Å longer than the corresponding Rh1−P_{ax} bond. Also, the equivalent elongations of the Rh2−S distances confirm that the multiple Rh2−S bond character, observed in precursor **1c**, disappears when atom Rh2 becomes octahedral in **4**. Since Rh1 is still unsaturated, the two sulfur bridges maintain or even strengthen their compensating electron donation toward this metal atom (somewhat shorter Rh1−S distances with respect to **1c**). Additionally, the H_2 molecule is almost staggered with respect to the four equatorial Rh−L bonds (the angle between the H−H−Rh plane and the Rh−Rh axis is 75°), but a single-point calculation of the structure where H_2 eclipses one Rh−S bond indicates a small energy increase of only 0.5 kcal mol^{-1}. The latter situation, which is important to trigger H_2 splitting, is easily accessible. A small rotation barrier is generally found for H_2 metal complexes by inelastic neutron scattering experiments, and the dependence from the coligand environment has been underlined.[29]

Before allowing a second H_2 molecule to be attracted by the still unsaturated Rh1 atom, we evaluated the possibility of cleaving the dihapto-coordinated H_2 molecule over one adjacent Rh−S bond. We optimized the geometry of the activation product $[RhHL_3(\mu\text{-}SH)(\mu\text{-}S)L_3Rh]^{2+}$, **5a** (top of Scheme 10),

Scheme 10

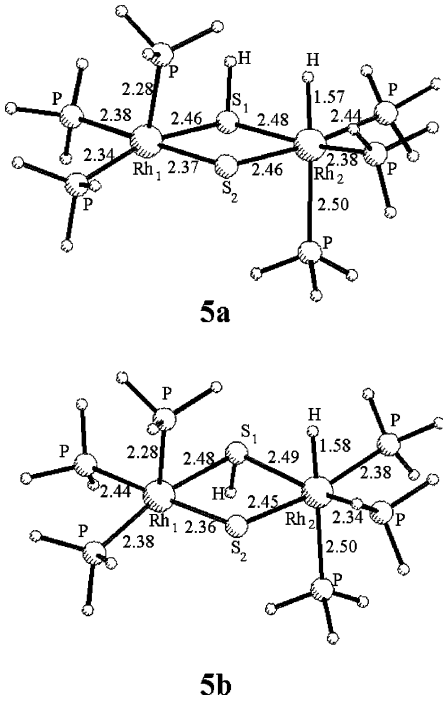

with the separated H atoms lying on the same side of the Rh_2S_2 plane.

An alternative isomer, **5b**, with the two H atoms above and below the Rh_2S_2 plane, is practically isoenergetic (only 0.5 kcal mol^{-1} higher than **5a**) and has very similar skeletal features. In both cases, all Rh−S bonds are elongated except for Rh1−S2, which does not involve any H atom (ca. 2.37 Å) and still can be attributed a bond order >1. The apical Rh−P bond, opposite the hydride ligand, is significantly elongated to 2.50 Å as a consequence of the known trans-influence exerted by terminal hydride ligands. This is noticeable also in the final product **2b** (Scheme 7) and in the corresponding experimental complex **2**. In these cases, however, the presence of a tripodal ligand mitigates somewhat the Rh−P_{ax} bond stretching (2.41 and 2.46 Å, respectively).

Conversion between isomers **5a** and **5b** was also studied in order to evaluate the associated energy cost. This was found to

Scheme 11

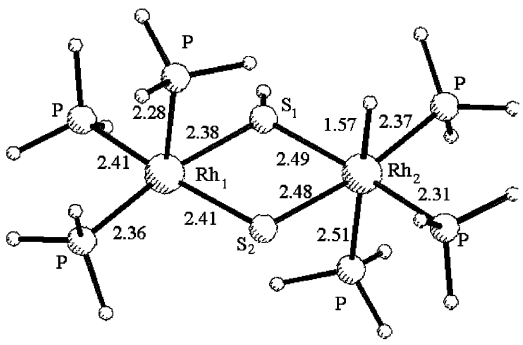

(28) Pidun, U.; Frenking, G. *Chem. Eur. J.* **1998**, *4*, 522.
(29) Eckert, J.; Kubas, G. J. *J. Phys. Chem.* **1993**, *97*, 2378.

be about 11 kcal mol^{-1} after the successful optimization of the transition state $\mathbf{5_{TS}}$, shown in Scheme 11. In the latter structure, the S−H bond lies in the Rh_2S_2 plane and, from the vibration of the imaginary frequency, the H atom is seen to move out of the Rh_2S_2 ring while staying in a plane perpendicular to it. Remarkably, the barrier is comparable with those of the hydrogenation pathway (vide infra), so that this flipping process of the hydrosulfido ligand may interfere at some point with the reformation of H_2, hence with its subsequent dissociation (recall the reversibility of the process). Such an event requires two adjacent H atoms.

An interesting structural observation is the quasi-equivalence of the Rh1−S1 and Rh1−S2 bonds in $\mathbf{5_{TS}}$, although they were significantly different in **5a** and **5b**. This is likely due to the return to planarity of S1, which, similar to S2, has a p_π orbital perpendicular to the Rh_2S_2 plane. Thus, π-bonding interactions with the metal Rh1 are equally possible for both S bridges.

Energetically, the H−H bond cleavage, with consequent transformation of the Rh(η^2-H_2) adduct **4** into the heterolysis product **5a**, is rather exothermic, the net energy gain being 15.8 kcal mol^{-1} (17.0 kcal mol^{-1} with respect to the separated reagents **1c** and H_2). Also, it has been possible to locate the transition state $\mathbf{4_{TS}}$ (see Scheme 12) for the conversion of **4** into **5a**. The barrier for hydrogen dissociation is 8.5 kcal mol^{-1} but is as large as 24.3 kcal mol^{-1} for the reverse H−H coupling, thus indicating that the latter require some drastic conditions such as those under a stream of nitrogen or other inert gas.[13]

Scheme 12

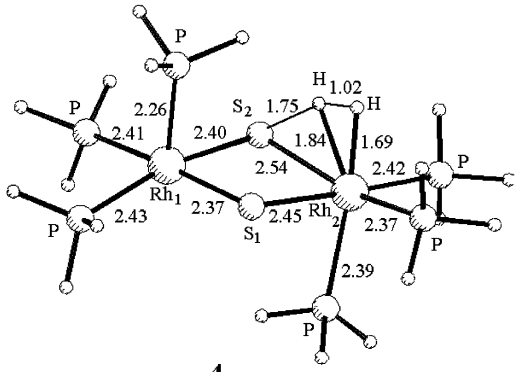

$\mathbf{4_{TS}}$

Notice that the H_2 molecule in $\mathbf{4_{TS}}$ is now coplanar with the Rh2−S2 vector. The H−H bond is significantly elongated (1.02 Å), and while one H atom almost occupies the sixth octahedral position of Rh2, the other H atom is already very close to the sulfur atom (1.75 Å). Also, a remarkable elongation of the subtended Rh2−S2 bond to 2.54 Å is observed together with some deformation from planarity of the $P_2RhS_2RhP_2$ skeleton.

In closing this section, we remark that the adjacent nucleophilic (sulfur) and electrophilic (rhodium) centers are indeed responsible for the heterolytic splitting of the dihydrogen molecule but not in the straightforward manner depicted in Scheme 8. First, H_2 is anchored in a side-on fashion at one metal and compensates for its electron deficiency with about 0.3 donated electrons. The induced positive charges render the H atoms more acidic, hence more suited to interact with one adjacent sulfur nucleophile. In the next section we will examine whether a second incoming H_2 molecule undergoes similar reaction conditions.

3.2. Access of the Second Dihydrogen Molecule. The attack can follow two alternative modes, namely, addition to the still unsaturated metal center may occur at either the η^2 monoadduct **4** or its derivative **5a**, where the first H_2 molecule is already split. Both the resulting structures, [Rh(η^2-H_2)L_3(μ-S)$_2L_3$(η^2-H_2)Rh]$^{2+}$, **6** (already hypothesized as an intermediate)[15] and [$RhHL_3$(μ-SH)(μ-S)L_3(η^2-H_2)Rh]$^{2+}$, **7**, have been found to be minima and are depicted in Scheme 13.

Scheme 13

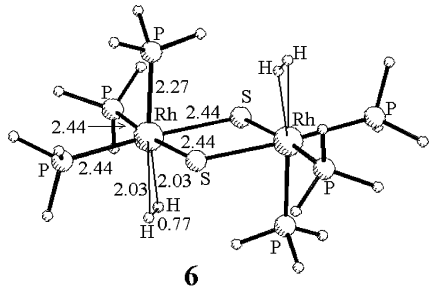

6

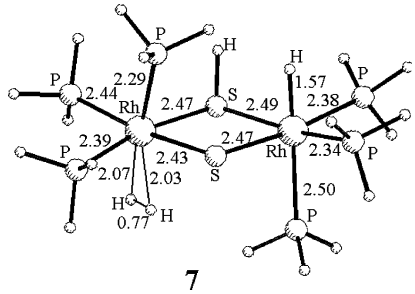

7

It may be assumed that the transition states to the latter species ($\mathbf{4'_{TS}}$ and $\mathbf{5a_{TS}}$, respectively) are very similar to $\mathbf{1c_{TS}}$ and that the activation energies are comparably small.

The transformation of the η^2-monoadduct **4** into the bisadduct **6** restores the symmetry of the Rh_2S_2 skeleton by equalizing all the Rh−S distances. The coordination of both H_2 molecules is less tight than in **4**, the Rh−H distances being about 0.1 Å longer. Less bonding to the metal also means stronger H−H bonds, and although the effects are small, the trend is evident. In fact, the shortest bond of 0.74 Å, observed in both the free dihydrogen and the very weak adduct of the transition state $\mathbf{1c_{TS}}$, increases to 0.77 and 0.78 Å in the bis- (**6**) and monoadducts (**4**), respectively.

In the alternative intermediate, **7**, the metal−hydride side of the molecule appears essentially unperturbed if compared with model **5a** while the Rh−($\eta^{2-}$$H_2$) interaction is as weak as in **6** (H−H distance of 0.77 Å) but more asymmetric (Rh−H distances of 2.03 and 2.07 Å, respectively). Moreover, the orientation of the H−H bond is not as in **4** since it almost eclipses the rhodium−sulfide linkage (HHRhS torsion of only 10°). The latter bond is equally long in **7** and **6** (∼2.44 Å), and no partial double-bond character may be assumed for it in either case. However, in **7** the sulfide ion is more negative (by about 0.05 e) than in species **1**, **4,** and **6**. The higher nucleophilicity is probably responsible for the reorientation of H_2 and suggests that H_2 heterolysis may proceed better from **7** than **6**.

From an energetic point of view, the side-on coordination of the second H_2 molecule follows a very flat potential-energy surface as it occurred for the first dihydrogen addition. The formation of **7** is computed to be slightly exothermic (−1.4 kcal

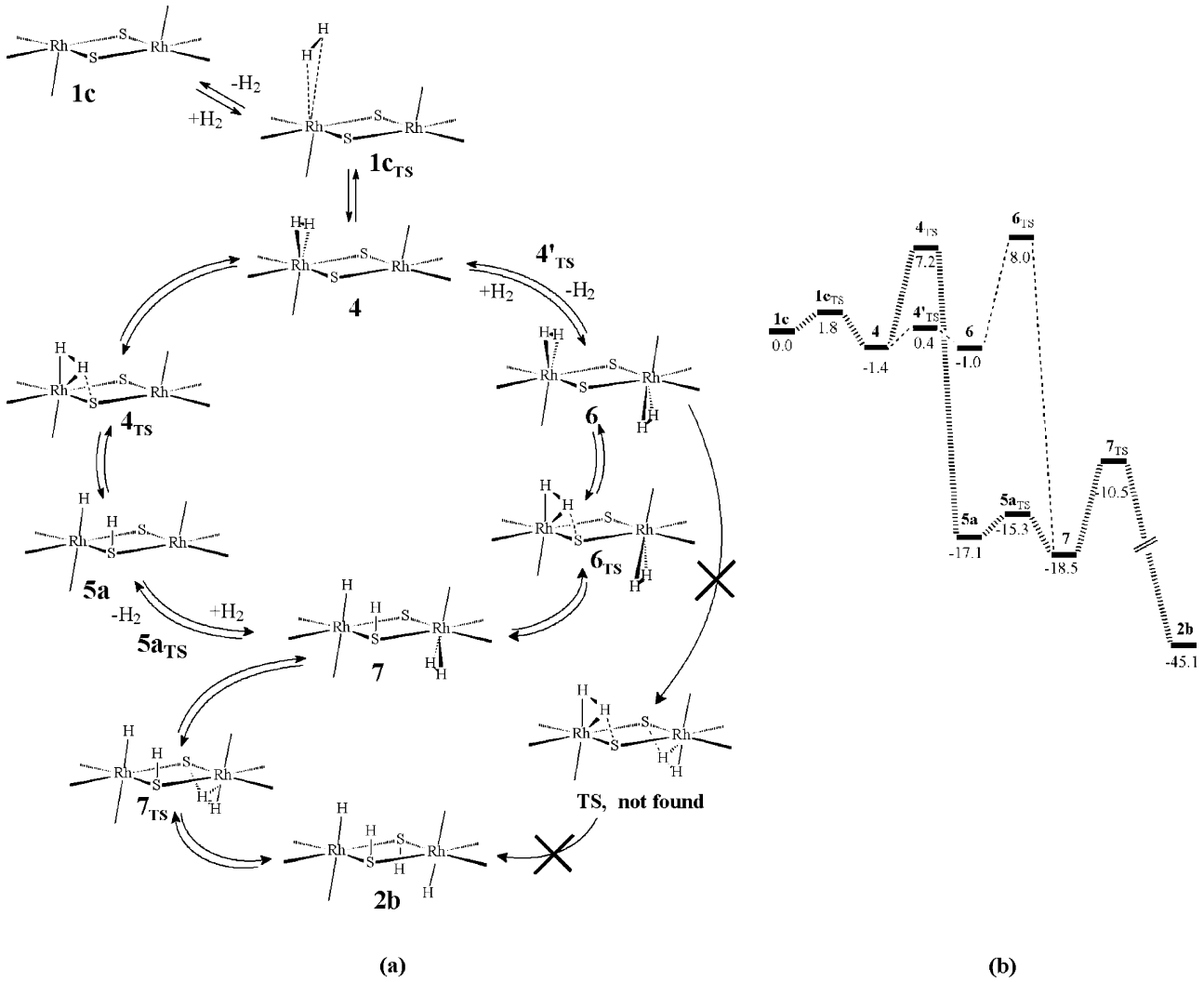

Figure 1. Flow chart (a) and energetic profiles (b) showing the calculated steps for the double heterolysis of two dihydrogen molecules over the Rh_2S_2 core. The transition states $\mathbf{4'_{TS}}$ and $\mathbf{5a_{TS}}$ are estimated from $\mathbf{1c_{TS}}$.

mol^{-1}) and that of **6** slightly endothermic (+0.3 kcal mol^{-1}). Whatever the meaning of these numbers, there is a hint that reaction through **6**, leading to a very unusual dimetallic bis-dihydrogen adduct, may be somewhat problematic, but it cannot be discarded on this basis.

3.3. Ultimate Conversion to the Final Product 2b. By determining the transition states that lead to **2b**, starting from either H_2 bisadduct **6** or **7**, further information on the reaction mechanism is obtained. Complex $\mathbf{6_{TS}}$ (upper Scheme 14) is the transition state between **6** and **7**, while $\mathbf{7_{TS}}$ (lower side) is the ultimate barrier to reach product **2b**.

The conceptually more difficult possibility that **2b** is obtained via the synchronous splitting of two dihapto-coordinated H_2 molecules (complex **6**) has been also tested. All of our computational efforts to optimize the corresponding transition state, as a centrosymmetric arrangement of two RhHHS units such as those in $\mathbf{4_{TS}}$, have been unsuccessful. Since there is no electronic underpinning for such a synchronizm and since the event would be again of the termolecular type, such a hypothesis can be dismissed.

By comparing the geometries of $\mathbf{6_{TS}}$ and $\mathbf{7_{TS}}$, the evolution of one RhHHS unit seems to be only marginally dependent on whether the first dihydrogen molecule is still intact or already

Scheme 14

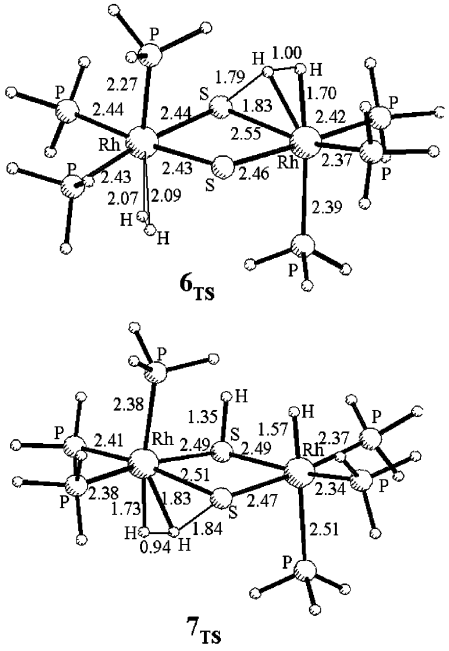

split. From an energetic viewpoint, heterolysis of the second H_2 molecule from the precursor **7** is significantly more exothermic than the first heterolysis from the precursor **6** (26.6 and 17.4 kcal mol^{-1} to obtain **2b** and **7**, respectively). On the other hand, the barrier at $\mathbf{7_{TS}}$ is only barely lower than that at $\mathbf{6_{TS}}$ (by ca. 1.0 kcal mol^{-1}).

3.4. Summary of the Overall Double-Hydrogenation Pathway. The various reaction steps with their respective transition states, which were described in detail above, are graphically summarized in Figure 1a, while Figure 1b provides the energetic profile of the entire reaction from **1c** to **2b**.

In the first step, one rhodium atom of the 32-electron precursor **1c** coordinates one H_2 molecule and forms the η^2-H_2 derivative **4**, going through $\mathbf{1c_{TS}}$ without a significant energy barrier. Complex **4** can either undergo the splitting of the coordinated dihydrogen, forming Rh−H and S−H new bonds and yielding complex **5a** (left side path of Figure 1a), or coordinate a second H_2 molecule to give the bis(dihydrogen) dimer **6** (right-side path). The mixed hydride−dihydrogen complex, **7**, can be obtained by either adding a second H_2 molecule to **5a** or splitting one of the coordinated H_2 molecules in **6**. Both pathways join together at **7**. In the final step, the second coordinated H_2 molecule also splits, affording the other set of Rh−H and S−H bonds in **2b**. A point to be made is that all the associative steps (H_2 additions) are disfavored by the entropy effects.

Since it was impossible to locate a transition state leading directly from the bis(dihydrogen) complex **6** to the final product **2b**, we conclude that the two dihydrogen molecules are activated one after the other. Conversely, it is not straightforward to establish, from our analysis, whether the second H_2 molecule adds to the dinuclear system before or after the splitting of the first one. As a matter of fact, the activation barriers for the two alternative transition states $\mathbf{4_{TS}}$ and $\mathbf{6_{TS}}$ leading to intermediates **5a** or **7**, respectively, have almost the same values (namely, 8.6 and 9.0 kcal mol^{-1}). Irrespective of the nature of the bimetallic precursor (**1c**, **5a**, or **4**) to which the dihydrogen molecule is added, the reaction (or its inverse) is energetically not very demanding (about 2 kcal mol^{-1}) and, therefore, cannot be the rate-determining step. Conversely, more energy is involved in the steps concerning dihydrogen splitting. In fact, the transition states $\mathbf{7_{TS}}$, $\mathbf{4_{TS}}$, and $\mathbf{6_{TS}}$ all determine very similar barriers of 8−9 kcal mol^{-1}, and it is not possible, on this basis, to identify the rate-determining step. On the other side, association of two dihydrogen molecules on precursor **1c** is disfavored by the entropy, and also the pathways through **6** should not be any better. By looking at the energy profile of Figure 1b and in keeping with the experimental finding for the real system, it is evident that **2b**, with two pairs of Rh−H and S−H bonds, is the most stable product of **1c** hydrogenation, but also intermediates **5a** and **7**, with only one pair of such linkages, are already much more stable than the separated reactants.

A further remarkable point concerns the reversibility of the reaction, i.e., the easy release of H_2 on purging a solution of the hydrogenated product(s) with nitrogen or argon. Computationally, the process is costly in terms of energy, with barriers of 35.1 and 22.9 kcal mol^{-1} for **2b** and **5a**, respectively. On the other hand, a favorable entropic contribution is predictable on account on the complex scission(s). Finally, the flow of inert gas would quickly eliminate H_2 from the environment, thus shifting the equilibrium toward precursor **1**.

The above computational results are not conclusive but provide useful hints about the evolution of the process. Accordingly, they have stimulated the need for additional experimental information concerning the actual nature of the intermediates. This has been looked at via careful reinvestigation of the in-situ NMR spectroscopy.

4. NMR Studies. 4.1. NMR Characterization of [(triphos)(H)Rh(μ-SH)$_2$Rh(H)(triphos)]$^{2+}$. The room-temperature ^{31}P-{^{1}H} NMR spectrum of the bis(hydrido)(μ-hydrosulfido) complex **2**, recorded in a 1:1 mixture of CD_2Cl_2/DMF-d_7, consists of a sharp doublet of triplets at −4.95 ppm and of a broad, featureless, resonance at ca. 23 ppm. The former signal is assigned to the phosphorus atom trans to the hydride ligand, while the latter, which integrates 2:1 with respect the higher field multiplet, can be ascribed to two exchanging phosphorus atoms coplanar with metal and sulfur atoms. A temperature increase to 55 °C gives rise to an AM_2X spin system (X = ^{103}Rh) that sharpens the low-field bump to a doublet of doublets at 21.4 ppm, while the other resonance remains almost unaffected, with only a slight high-field shift (δ −5.05 ppm). The lowering of the temperature to −50 °C freezes the exchange process in line with the presence of two magnetically inequivalent phosphorus atoms trans to the SH ligands, and as soon as the slow-exchange regime is attained, the spectrum changes to a well-resolved AMQX spin system (see the Experimental Section and the spectrum which is reported as Supporting Information).

The ^{1}H NMR spectrum, recorded at room temperature in the same solvent mixture, shows, apart from the uninformative triphos resonances, two distinct high-field signals centered at −2.12 and −5.80 ppm. These signals have the same intensity and integrate 1:3 with respect to the methyl proton of triphos resonating at 2.02 ppm. The more upfield resonance, assigned to the terminal hydride ligand coordinated to the rhodium atom ($J_{HPtrans}$ = 185.0 Hz), consists of a broad doublet, whereas the other signal, appearing as a broad almost unresolved triplet (J_{HP} ca. 14 Hz), is ascribed to the bridging hydrosulfide. A similar value of the SH chemical shift was reported for the dinuclear rhodium hydrosulfido complex [{Cp*Rh}$_2$(μ-CH$_2$)$_2$(μ-SH)]$^+$.[30] Temperature lowering down to −50 °C slightly sharpens both resonances without providing any fine structure for the hydride resonance.

4.2. In Situ NMR Analysis of the Hydrogenation Reaction of 1. To gain insight into the mechanism that rules the addition of dihydrogen to the Rh_2S_2 complex **1**, we decided to follow the reaction in situ by NMR spectroscopy. A solution of **1**, in a 1:1 mixture of CD_2Cl_2/DMF-d_7, was saturated with H_2, and the progress of the reaction was monitored by ^{31}P and ^{1}H NMR spectroscopy. As the hydrogenation of **1** is relatively slow, even at room temperature and an atmospheric pressure of H_2, the experiments were carried out by pressurizing the NMR tube, precooled at −78 °C, with two atm of H_2 (5 mm Wilmad NMR tube with J Young valve). Higher pressures of dihydrogen (up to 50 atm), tested inside a titanium-headed sapphire NMR tube,[31] slightly increased the reaction rate but did not affect the nature

(30) Kaneko, Y.; Suzuki, N.; Nishiyama, A.; Suzuki, T.; Isobe, K. *Organometallics* **1998**, *17*, 4875. Godziela, G.; Tonker, T.; Rakowski DuBois, M. *Organometallics* **1989**, *8*, 2220.

of the hydrogenation products and, more importantly, did not provide additional mechanistic information.

In the $^{31}P\{^1H\}$ NMR spectrum recorded at −78 °C, the sharp doublet of complex **1** centered at ca. 26.1 ppm (J_{PRh} 103.5 Hz) does not change, thus indicating that the compound does not add dihydrogen. Only at −50 °C does a slow reaction take place, resulting in the uptake of only one molecule of H_2 (the spectroscopic features are very different from those of **2**) and the formation of an intermediate defined as **3**. This species shows a broad resonance at ca. 23 ppm, which does not resolve into a fine structure after cooling the probe head down to −80 °C, the lowest accessible temperature with the mixture of solvents used. At this extreme temperature **3** gives rise to a broad resonance at ca. 25 ppm accompanied by a broad hump at −14 ppm, which indicates a system still far away from the slow-exchange regime. The persisting fluxional behavior of **3** at low temperature may account for the existence of a low-energy equilibration of the ligands around the Rh_2S_2 core. In particular, this could imply transfer of the H ligand between the S,SH-bridged metals, the details of the possible mechanism being provided in section 5. Notice that in this case there is no evidence of the fast S−H···S proton transfer which occurs in the dinuclear platinum complex $[Pt_2\{Ph_2P(CH_2)_3PPh_2\}_2(\mu\text{-S})(\mu\text{-SH})]ClO_4$ and has been experimentally and theoretically analyzed by Aullón et al.[32]

Important information is also provided by the proton NMR spectrum. At −45 °C, as soon as the hydrogenation of **1** starts, two resonances of equal intensities grow in the negative part of the ^1H NMR spectrum (namely, a relatively neat singlet at −1.24 ppm ($w_{1/2}$ = 7.4 Hz) and a multiplet centered at ca. −6.03 ppm). The higher field multiplet is not sharp and may be interpreted as a doublet of triplets with J_{HP} = 61.5 and 33.5 Hz, respectively (Figure 2, trace a). The broadening is probably a consequence of unresolved couplings to both rhodium nuclei and to other phosphorus atoms located further away from the hydride ligand. Further cooling of the solution does not change this picture, and the hydride signal does not resolve into a fine multiplet.

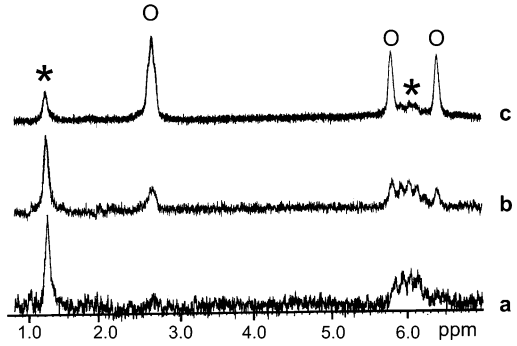

Figure 2. ^1H NMR spectra in the high-field region for the reaction between **1** and H_2 (2 atm), which show the hydride and the hydrosulfide resonances of compounds **3** (—) and **2** (**O**). (a) Spectrum taken after 10 min at −45 °C. (b) Spectrum taken after 40 min at −45 °C. (c) Spectrum taken after 150 min at −45 °C (299.94 MHz, CD_2Cl_2/DMF-d_7).

Analysis of the spectroscopic properties of the intermediate hydrogenation product **3** is complicated because this species, as soon as it is formed, starts to transform into final product **2** at a comparable rate (Figure 2, trace b). As a matter of fact, after 2 h at −45 °C, the transformation into final complex **2**, which evidently originates from **3** through addition of a second H_2 molecule, is almost complete (Figure 2, trace c). At higher temperatures the transformation of **3** into **2** is faster, so that no appreciable concentration of the intermediate is detected when monitoring the reaction above −10 °C.

The η^2-H_2 coordination mode in **3** can be safely ruled out from analysis of the spin−lattice relaxation times measured through the inversion−recovery method at 300 MHz. Thus, at −45 °C, the singlet at −1.24 ppm shows a T_1 of 466 ms and the higher field multiplet exhibits a similar relaxation (T_1 = 507 ms). These values, in turn, compare well with those measured for **2** in the same conditions of temperature and magnetic field ($T_{1(\mu-SH)}$ = 690 ms; $T_{1(Rh-H)}$ = 417 ms), while the times are much longer than those expected for a genuine molecular dihydrogen complex.[33] In this respect, it is worth mentioning that the complex $[(triphos)Rh(H)_2(\eta^2\text{-}H_2)]^+$, which is stable at low temperature, features a fast spinning H_2 ligand with T_{1min} = 38.9 ms (in CD_2Cl_2 at 220 K and 400 MHz).[34] The latter value (after scaling down to ca. 29 ms at 300 MHz to match the magnetic field used in the relaxation measurements of **3**) is definitely smaller than those measured for the two high-field resonances of **3**.

In summary, the NMR data are consistent with **3** being a dinuclear species which contains new SH and H ligands with respect to precursor **1**. The compound, which is a rare example of an interceptable mono-dihydrogenated intermediate in an overall bis-dihydrogenation process, could possibly correspond to the model species **5a** (left-side path in Figure 1a) which contains a terminal hydride ligand. Such an interpretation may be in contrast somewhat with the lack of a large upfield resonance expected for a terminal hydride trans to one phosphorus donor. On the other hand, the possibility that the hydride ligand lies in a bridging position between the metals cannot be completely excluded, although no high-field signal, safely attributable to such a hydride, is observed. Further considerations on the point are presented in section 5.

4.3. Para-H_2 Effects in the Hydrogenation of 1. In recent years, several applications of the para-H_2 effects in NMR spectroscopy have been reported, mostly dealing with characterization of solution structures of species which are present in very low concentration[35] and elucidation of reaction mechanisms.[35,36] This phenomenon arises from the great enhancement of the proton NMR transitions in the hydrogenated product, provided that hydrogenation originates from para-H_2 and the spin correlation between the transferred protons is maintained. Methods employing direct and indirect population transfers in conjunction with para-H_2 have been successfully applied also to enhance the corresponding heteronucleus population such as ^{13}C, ^{31}P, ^{103}Rh, ^{195}Pt.[36] Therefore, use of para-hydrogen in examining the current reaction may be important for detection

(31) Bianchini, C.; Meli, A.; Moneti, S.; Oberhauser, W.; Vizza, F.; Herrera, V.; Fuentes, A.; Sanchez-Delgado, R. *J. Am. Chem. Soc.* **1999**, *121*, 7071. Bianchini, C.; Freudiani, P.; Meli, A.; Vizza, F. *Chem. Ber./Recl.* **1997**, *130*, 1633. Bianchini, C.; Meli, A.; Traversi, A. Italian Patent FI A000025, 1997.
(32) Aullón, G.; Capdevila, M.; Clegg, W.; Gonzales-Duarte, P.; Llenos, A.; Mas-Ballesté, R. *Angew. Chem., Int. Ed.* **2002**, *41*, 2776.
(33) Hamilton, D. G.; Crabtree, R. H. *J. Am. Chem. Soc.* **1989**, *110*, 4126.
(34) Bakhmutov, V. I.; Bianchini, C.; Peruzzini, M.; Vizza, F.; Vorontsov, E. V. *Inorg. Chem.* **2000**, *39*, 1655.
(35) (a) Duckett, S. B. In *Recent Advances in Hydride Chemistry*; Peruzzini, M., Poli, R., Eds.; Elsevier SA: Amsterdam, The Netherlands, 2001; Chapter 11. (b) Duckett, S. B.; Sleigh, C. J. *Prog. Nucl. Magn. Spectrosc.* **1999**, *34*, 71 and references therein.
(36) Aime, S.; Gobetto, R.; Canet, D. *J. Am. Chem. Soc.* **1998**, *120*, 6770.

of early reaction intermediates. In the present case, we observe that in the intermediate and final products (**3** and **2**, respectively) the spin correlation between the two para-hydrogen protons is not maintained, i.e., the *J* coupling is too small. As a consequence, no hyperpolarization effect is expected in these molecules. The resonances, readily assigned to complex **3**, slowly decrease, and the gradual formation of the signals associated to the compound **2** is observed. This information supports the hypothesis that compound **3** corresponds to structure **5a** and the second hydrogen addition proceeds through this intermediate and does not involve a bis(η^2−H_2) adduct.[37] The lack of polarized signals excludes the occurrence of an oxidative addition in the formation of **2** from the nonclassical putative intermediate **4**. Rather, it suggests that a sulfur-assisted heterolytic splitting of the rhodium-coordinated H_2 molecule over the Rh−S polarized bond is the most feasible process which accounts for the formation of **3** from **1** and, alternately, that of **2** from **3**.

5. Further Theoretical Studies. The computational results, outlined in Figure 1a, may be reconsidered in light of the spectroscopic analysis, which in turn provides some hints for supplementary computations. First, the para-hydrogen experiments confirm that no oxidative addition process takes place at the metal atoms to give metal−dihydride species. On the other hand, there is no spectroscopic evidence of the Rh−(η^2−H_2) adducts **4**, **6,** or **7** which may have a lifetime that is too short to be detected. NMR indication of only one stable intermediate between **1** and **2** (compound **3**, possibly identified with **5a**) discards the formation of **6** with two coexisting Rh−(η^2-H_2) moieties. In this case and by referring to Figure 1a, the subsequent formation of **7** would lead, preferentially, to final product **2b**, while **5a** would be only a side product. Moreover, both hydrogen reactants would be adsorbed at once and not stepwise, as indicated by the NMR analysis. In conclusion, the unlikeness of a termolecular reaction is confirmed.

The most intriguing aspect of the NMR study is the equivalence of all the phosphorus nuclei in intermediate **3** which persists even at −80 °C. If the latter species indeed corresponded to **5a**, a mechanism interchanging the octahedral and five-coordinated metal centers should be operative. Scheme 15 shows two possible routes for the transfer of the hydride ligand between the metals, namely, through the formation of a (μ-sulfido)(μ-dihydrosulfide), **5c**, or of a bis(μ-dihydrosulfide), **5d**, bridged system. Notice that both are affected by a conceptual drawback which concerns a change of both the metal oxidation state [Rh(III) → Rh(II) → Rh(III)] and the nature of the transferring H atom (hydride → proton → hydride). From an energetic point of view, the necessary flipping of the S−H bond, below the Rh_2S_2 plane and opposite to the Rh−H linkage, has a relatively low energy cost (only 11 kcal mol^{-1} to reach $\mathbf{5_{TS}}$ reported in Scheme 11).

An attempted optimization of **5c** indicated that one of the two Rh−S(H_2) bonds is broken and clearly dismissed the route.

Scheme 15

5c **5d**

Conversely, structure **5d** could be optimized as a real minimum with energy about 12.3 kcal mol^{-1} higher than that of **5a**, a value which can be consistent with fluxional behavior.

There is however a third possible way of dynamically equalizing the two metal centers which requires significant structural rearrangements. The key species **5e** (see the optimized structure in Scheme 16) combines μ-sulfido, μ-hydrosulfide, and μ−hydrido bridges and corresponds to a stable stationary point with an energy about 11.6 kcal mol^{-1} lower than the isomer **5a**.

Scheme 16

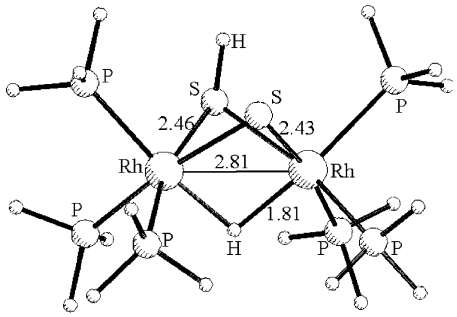

5e

A comparable iridium complex, $(PPh_3)_2HIr(\mu\text{-}S)(\mu\text{-}SH)(\mu\text{-}H)IrH(PPh_3)_2$, was characterized by Pignolet et al.[38] and isolated by Rauchfuss et al.[19] as the final product of the double hydrogenation of the diiridium(II) species $(PPh_3)_2Ir(\mu\text{-}S)_2Ir(PPh_3)_2$. In our case, the thermodynamic stability of **5e** is also consistent with the lack of a major steric problem between triphos ligands (for instance, $[(triphos)Fe(\mu\text{-}H)_3Fe(triphos)]^+$ is perfectly stable despite the very short Fe−Fe distance of 2.33 Å[39]). On the other hand, it is questionable whether the equivalent of **5e**, with two terminal triphos ligands, is kinetically consistent with the hydrogenation process which occurs also in the solid state.[40] In fact, the reversible rearrangement of **5a** into **5e** requires not only the staggered to eclipsed transformation of the fragment (triphos)Rh(μ-S)$_2$Rh(triphos), but also easy puckering and unpuckering of the overall framework. These rearrangements are most likely incompatible with the rapid scrambling process and the solid-state reactivity, for which there is little doubt that **5a** must be the active species for the second H_2 addition. As another consideration, the reverse dehydrogenation process would become energetically rather difficult if **5e** was the actual intermediate to start from. In fact, one should add the **5e** stabilization energy (11.6 kcal mol^{-1}) to the already high barrier from **5a** to $\mathbf{4_{TS}}$ (24.3 kcal mol^{-1}, see Figure 1b).

In conclusion, the calculations following the NMR study have helped to frame the stereochemical and energetic problems associated with the fluxionality of the observed intermediate **3**. On one hand, the bridged hydride species **5e** would fully explain the equivalence of all the P donors as well as the lack of a large J_{HP} coupling of the metal hydride with the trans P donor. On the other hand, the fluxionality through intermediate **5d** has reasonable energetic costs but implies a new and unusual case

(37) A second experiment carried out a slightly similar temperature (−45 °C) closely reproduced that performed at −50 °C.
(38) Mueting, A. M.; Boyle, P. D.; Wagner, R.; Pignolet, L. H. *Inorg. Chem.* **1988**, *27*, 271.
(39) Dapporto, P.; Midollini, S.; Sacconi, L. *Inorg. Chem.* **1975**, *14*, 1643.
(40) There is no evidence for reversibility of the process in this case.

of reductive elimination mechanism. Although the calculations and the experimental data are not conclusive about the actual nature of **3**, a possible explanation is the coexistence, at least in solution, of both species **5a** and **5e** when the double-dihydrogenation process is halfway.

Conclusions

The combined theoretical and experimental studies have shown that the electronically unsaturated Rh_2S_2 dimeric framework (**1**), thanks to the unique proximity of electrophilic metal centers and nucleophilic sulfur atoms, is able to add and split heterolytically two dihydrogen molecules in a stepwise fashion. In this case, the process compares but it is not exactly equal to a σ-bond metathesis (proposed by other authors[12]), since the newly formed Rh−H and S−H bonds stem from σ(H−H) and π(Rh═S) bonds. On the other hand, a strict similarity is noticed with the hydrogenation occurring over a Ru═N bond, as experimentally and computationally defined by Morris.[41] Importantly, our presented mechanism is intrinsically different from that reported by Rauchfuss et al. for the related Ir_2S_2 core, which implies two different modes of H_2 activation.[19] While the latter system remains to be explored with the powerful tools of theoretical chemistry, our calculations for the present Rh_2S_2 system indicate that each H_2 molecule must be first tightly anchored by one metal in a side-on coordination mode (a feature not experimentally detectable) and confirm that the heterolytic splitting precedes the addition of the second H_2 molecule, which undergoes in turn a very similar activation mechanism.

Finally, as a remarkable result of this study, NMR spectroscopic analysis of a double-dihydrogenation process has allowed intercepting a rare halfway intermediate of the reaction.

Experimental Section

1. General Notes. All reactions and manipulations were routinely performed under a nitrogen or argon atmosphere by using standard Schlenk techniques. Reactions under a controlled pressure of hydrogen were performed with a stainless steel Parr 4565 reactor (100 mL) equipped with a Parr 4842 temperature and pressure controller. CH_2Cl_2 and DMF were purified by distillation from $LiAlH_4$ and CaH_2 respectively. Infrared spectra were recorded on a Perkin-Elmer 1600 series FT-IR spectrophotometer using samples mulled in Nujol between KBr plates. Elemental analyses (C, H, N) were performed using a Carlo Erba Model 1106 elemental analyzer. [(triphos)RhCl(C_2H_4)] was prepared as previously described.[42]

2. NMR Experiments. NMR studies were carried out in standard 5 mm Wilmad NMR tube with J Young valve containing solutions of the complexes in 1:1 CD_2Cl_2/DMF-d_7 mixtures (ca.1 $\times$ 10^{-2} mmol). The tube was frozen at −100 °C with a liquid nitrogen/acetone bath and then pressurized with hydrogen to ca.2 atm. Both ^{1}H and ^{31}P{^{1}H}-NMR spectra were recorded in the temperature range from −80 to 25 °C.

Deuterated solvents for NMR measurements (Aldrich) were dried over molecular sieves (4 Å). ^{1}H NMR spectra were recorded on a Varian VXR300 spectrometer operating at 299.94 MHz. Peak positions are relative to tetramethylsilane and calibrated against the residual solvent resonance of CD_2Cl_2 (δ = 5.33). ^{31}P{^{1}H}NMR spectra were recorded on the same instrument operating at 121.42 MHz. Chemical shifts were measured relative to external 85% H_3PO_4 with downfield values taken as positive.

The conventional inversion−recovery method ($180° \angle \tau \angle 90°$) was used to determine the variable-temperature longitudinal-relaxation time T_1. Calculation of the relaxation times was made using the nonlinear three-parameter fitting routine of the spectrometer. In each experiment, the waiting period was 5 times longer than the expected relaxation time and 10−16 variable delays were employed. The duration of the pulses was controlled at each temperature. The errors in T_1 determinations were lower than 10% (this was checked with different samples).

The high-pressure NMR (HPNMR) experiments were performed in 10-mm sapphire tubes (Saphikon Inc., NH) assembled with Ti-alloy pressure heads constructed at ICCOM-CNR.[31] The HPNMR spectra were recorded by using a standard 10-mm probe tuned to ^{31}P and ^{1}H nuclei on a BRUKER AC 200 spectrometer operating at 81.01 MHz. **CAUTION:** *All manipulations involving high pressures are potentially hazardous. Safety precautions must be taken at all stages of NMR studies involving high-pressure tubes.*

The ^{1}H−PHIP NMR spectra were recorded on a JEOL EX 400 spectrometer at a proton resonance frequency of 400 MHz. The hydrogenation reactions conducted inside of the NMR magnet were performed at 25 °C using a conventional ^{1}H-multinuclear probehead. Para-H_2 (50% enriched in the para-form) was prepared according to the published method.[43]

In a typical experiment using hyperpolarized hydrogen, 10 mg of **1** (4.7×10^{-3} mmol) was dissolved in 0.6 mL of a 1:1 (v/v) CD_2Cl_2/DMF-d_7 mixture in a 5 mm resealable NMR tube having a total volume of 3 mL. The solution was frozen, the air was pumped-off, and about 1 atm of para-H_2 cooled at −196 °C was added. The sample was then warmed to the desired temperature (−50 and −45 °C, in two separate experiments), vigorously shaken, and then introduced into the spectrometer. The first spectrum was recorded ca. 15 s after shaking of the sample.

3. Synthesis of the Complexes. 3.1. Synthesis of [(triphos)HRh-(μ-SH)$_2$RhH(triphos)](BPh$_4$)$_2$ (2). Complex **2** was obtained from a modification of the synthesis originally reported.[13] To a solution of [(triphos)RhCl(C_2H_4)] (0.4 g, 0.5 mmol) in CH_2Cl_2 (25 mL), H_2S was gently bubbled for 5 min at room temperature.[44] When the color of the solution changed from orange to yellowish brown, the H_2S was replaced with a stream of nitrogen. A solution of $NaBPh_4$ (0.25 g, 0.73 mmol) in ethanol (30 mL) was slowly added with stirring. Partial evaporation of the solvent under nitrogen led to separation of a pink microcrystalline product, which was collected by filtration and washed with ethanol (3 $\times$ 5 mL) and pentane (3 $\times$ 5 mL) before being dried under a stream of nitrogen. Yield: 0.48 g, 90%. Anal. Found (calcd) for $C_{130}H_{82}P_6S_2Rh_2$: C, 74.82 (74.36); H, 4.13 (3.94).

IR (Nujol; cm^{-1}): ν = 2540 ν(SH), 2010 ν(RhH). ^{31}P{^{1}H} NMR (121.4 MHz, DMF-d_7/CD_2Cl_2 (1:1, v/v), AM_2X spin system at 25 °C (X = ^{103}Rh): δ −4.75 (dt, P_A, J_{PAPM} 23.2 Hz, J_{PARh} 71.3 Hz); 23 (brd, P_M). AM_2X spin system at 55 °C: δ −5.05 (dt, P_A, J_{PAPM} 22.0 Hz, J_{PARh} 71.5 Hz), 21.4 (dd, P_M, J_{PMRh} 100.1 Hz). AMQX spin system at −50 °C: δ −4.04 (dt, P_A, J_{PAPM} 22.0 Hz, J_{PAPQ} 22.0 Hz, J_{PARh} 71.5 Hz), 9.92 (ddd, P_M, J_{PMPQ} 5 Hz, J_{PMRh} 101.8 Hz), 32.1 (ddd, P_Q, J_{PQRh} 100.4 Hz.^{1}H NMR (299.94 MHz, DMF-d_7/CD_2Cl_2 (1:1, v/v, 25 °C): δ 6.8−7.9 (m, H aryl), 3.0−3.4 (br, 6H, CH_2P), 2.02 (br, 3H, CH_3C), −2.12 (brt, 2H, SH, J_{HP} 14 Hz), −5.8 (brd, 2H, RhH, $J_{HPtrans}$ 185 Hz).

3.2. Synthesis of [(triphos)Rh(μ-S)$_2$Rh(triphos)](BPh$_4$)$_2$ (1). The complex was obtained from a modification of the synthesis originally reported.[44] A stream of argon was bubbled for 30 min throughout a solution of **2** (0.15 g, 0.07 mmol) in CH_2Cl_2 (20 mL) and DMF (10 mL) at room temperature. During this time the color of the solution changed from orange to reddish brown. *n*-Butanol (3 mL) and *n*-dibutyl ether (30 mL) were then added. On standing, a red-brown microcrys-

(41) Abdur-Rashid, K.; Clapham, S. E.; Hadzovic, A.; Harvey, J. N.; Lough, A. J.; Morris, R. H. *J. Am. Chem. Soc.* **2002**, *124*, 15104.
(42) Bianchini, C.; Meli, A.; Mealli, C.; Sabat, A. *J. Chem. Soc., Chem. Commun*. **1986**, 778.
(43) Aime, S.; Dastù, W.; Gobetto, R.; Reineri, F.; Russo, A.; Viale, A. *Organometallics* **2001**, *20*, 2924.
(44) (a) Bianchini, C.; Meli, A.; Laschi, F.; Vizza, F.; Zanello, P. *Inorg. Chem*. **1989**, *28*, 277. (b) Bianchini, C.; Meli, A.; Laschi, F.; Vacca, A.; Zanello, P. *J. Am. Chem. Soc.* **1988**, *110*, 3913.

talline product was formed, which was filtered off and washed with *n*-butanol (3 × 5 mL) and pentane (3 × 5 mL) before being died under a stream of nitrogen. Yield: 0.1 g, 70%. Anal. Found (calcd) for $C_{130}H_{78}P_6S_2Rh_2$: C, 74.50 (74.25); H, 3.75 (3.52). $^{31}P\{^1H\}$ NMR (121.4 MHz, DMF-d_7/CD_2Cl_2 (1:1, v/v), 25 °C) A_3X spin system (X = ^{103}Rh): δ 24.5 (d, P_A, J_{P-Rh} 103.54 Hz). ^1H NMR (299.94 MHz, DMF-d_7/CD_2Cl_2 (1:1, v/v), 25 °C): δ 6.6−7.4 (m, H ar), 2.8 (br, 6H, CH_2P), 1.6 (br, 3H, CH_3C).

3.3. Alternative Syntheses of [(triphos)HRh(μ-SH)$_2$RhH(triphos)](BPh$_4$)$_2$ (2) by Hydrogenation of 1. (a) In Solution. A solution of **1** (0.1 g, 0.047 mmol) in CH_2Cl_2 (30 mL) and DMF (10 mL) was treated with a stream of H_2 for 30 min at room temperature. The color of the solution changed from orange to reddish brown within 10 min. On addition of ethanol (30 mL), pink crystals of **1** precipitated, which were collected by filtration and washed with ethanol and pentane. Yield: 0.09 g, 90%.

(b) In the Solid State. A solid sample of **1** (0.1 g, 0.047 mmol) was placed in a Teflon vessel inside a 100 mL Parr reactor which was evacuated with three vacuum/nitrogen cycles and then pressurized with 40 atm of H_2. The reactor was maintained at room temperature for 24 h and then slowly depressurized. The solid was quickly transferred in a Schenk flask and filled with nitrogen. $^{31}P\{^1H\}$ and ^1H NMR spectra of the crude product showed only a 30% conversion to **1**.

4. Computational Details.

The structural optimizations were carried out at the hybrid density functional theory (DFT) by using the Becke's three-parameter hybrid exchange-correlation functional[45] with the nonlocal gradient correction of Lee, Yang, and Parr (B3LYP)[46] using the Gaussian98 suite.[47] The nature of all optimized structures was confirmed by calculation of the frequencies. Concerning the strategies for searching transition-state structures, we briefly illustrate what was done for the point $\mathbf{4_{TS}}$ (refer to Figure 1a). After localizing the stationary points **1c**, **7**, the QST2 method was adopted by requesting at the same time the simultaneous optimization, in redundant internal coordinates, of TS and five additional points along the path joining **1c** and **7.**[48] To reduce computational time, the latter calculations were performed using the HF method and a small basis set. After the successful identification of the transition state, its structure was optimized again by adopting the usual higher level model chemistry.

A collection of Cartesian coordinates and total energies for all optimized molecules is available from the authors upon request. The ruthenium, phosphorus, and sulfur atoms were calculated using the effective core potentials of Hay and Wadt.[49] The basis set for the metal atoms is the double-ζ valence basis functions associated with the ECP of Hay and Wadt.[50] The basis set used for the remaining atomic species was the 631G (d,p) for all atoms.[50]

For the EHMO calculations[51] and the graphical analysis of the results, the package CACAO[52] was used.

Acknowledgment. M.P. wishes express his gratitude to INTAS (00-00179) and EC (RTN HYDROCHEM, HPRN-CT-2002-00176) for promoting this scientific activity and financial support. This work was also supported by "Firenze Hydrolab" through a generous grant by Ente Cassa di Risparmio di Firenze. The collaboration between the ICCOM and ITQB Institutes has been made possible thanks to the bilateral program CNR-GRICES. The grant provided by CINECA for the usage of the package Gaussian98 and for free computing time is kindly acknowledged by C.M. and A.I.

Supporting Information Available: Electronic interpretation of the lower stabilization energy of conformer **1d** vs **1c** as well as the NMR spectra of compound **2** registered at different temperatures. This material is available free of charge via the Internet at http://pubs.acs.org.

JA047992J

(45) Becke, A. D. *J. Chem. Phys.* **1993**, *98*, 5648.
(46) Lee, C.; Yang, W.; Parr, R. *Phys. Rev. B* **1988**, *37*, 785.
(47) Frisch, M. J.; Trucks, G. W.; Schlegel, H. B.; Scuseria, G. E.; Robb, M. A.; Cheeseman, J. R.; Zakrzewski, V. G.; Montgomery, J. A., Jr.; Stratmann, R. E.; Burant, J. C.; Dapprich, S.; Millam, J. M.; Daniels, A. D.; Kudin, K. N.; Strain, M. C.; Farkas, O.; Tomasi, J.; Barone, V.; Cossi, M.; Cammi, R.; Mennucci, B.; Pomelli, C.; Adamo, C.; Clifford, S.; Ochterski, J.; Petersson, G. A.; Ayala, P. Y.; Cui, Q.; Morokuma, K.; Malick, D. K.; Rabuck, A. D.; Raghavachari, K.; Foresman, J. B.; Cioslowski, J.; Ortiz, J. V.; Stefanov, B. B.; Liu, G.; Liashenko, A.; Piskorz, P.; Komaromi, I.; Gomperts, R.; Martin, R. L.; Fox, D. J.; Keith, T.; Al-Laham, M. A.; Peng, C. Y.; Nanayakkara, A.; Gonzalez, C.; Challacombe, M.; Gill, P. M. W.; Johnson, B. G.; Chen, W.; Wong, M. W.; Andres, J. L.; Head-Gordon, M.; Replogle, E. S.; Pople, J. A. *Gaussian 98*, revision A.9; Gaussian, Inc.: Pittsburgh, PA, 1998.
(48) Ayala, P. Y.; Schlegel, H. B. *J. Chem. Phys.* **1997**, *107*, 375.
(49) (a) Dunning, T. H., Jr.; Hay, P. J. *Modern Theoretical Chemistry*; Plenum: New York, 1976; p 1. (b) Hay, P. J.; Wadt, W. R. *J. Chem. Phys.* **1985**, *82*, 299.
(50) Hariharan, P. C.; Pople, J. A. *Theor. Chim. Acta* **1973**, *28*, 213.
(51) (a) Hoffmann, R.; Lipscomb, W. N. *J. Chem. Phys.* **1962**, *36*, 2872. (b) Hoffmann, R.; Lipscomb, W. N. *J. Chem. Phys.* **1962**, *37*, 3489.
(52) (a) Mealli, C.; Ienco, A.; Proserpio, D. M. *Book of Abstracts of the XXXIII ICCC*; Florence, 1998; p 510. (b) Mealli, C.; Proserpio, D. *J. Chem. Educ.* **1990**, *67*, 399.